European Research Infrastructure supporting Smart Grid and Smart Energy Systems Research, Technology Development, Validation and Roll Out – Second Edition

Project Acronym: **ERIGrid 2.0**

Project Number: **870620**

Technical Report Lab Access User Project

Fault TroubleShooter (FaultTS)

Access Duration: 06/02/2023 to 10/02/2023

Funding Instrument:	Research and Innovation Action
Call:	H2020-INFRAIA-2019-1
Call Topic:	INFRAIA-01-2018-2019 Integrating Activities for Advanced Communities
Project Start:	1 April 2020
Project Duration:	54 months
User Group Leader:	José Oliveira (ENEIDA.IO)

This project has received funding from the European Union's Horizon 2020 research and innovation programme under Grant Agreement No. 870620.

Report Information

Document Administrative Information	
Project Acronym:	ERIGrid 2.0
Project Number:	870620
Access Project Number:	158
Access Project Acronym:	FaultTS
Access Project Name:	Fault TroubleShooter
User Group Leader:	José Oliveira (ENEIDA.IO)
Document Identifier:	ERIGrid2-Report-Lab-Access-User-Project-FaultTS-final
Report Version:	v1.0
Contractual Date:	10/04/2023
Report Submission Date:	14/04/2023
Lead Author(s):	João Campos
Co-author(s):	Guilherme Freire, José Oliveira
Keywords:	Low Voltage (LV) networks, faults, short-circuits, European Union (EU), H2020, Project, ERIGrid 2.0, GA 870620
Status:	__ draft, _x_ final

Change Log

Date	Version	Author/Editor	Summary of Changes Made
14/04/2023	v1.0	João Campos	Final Version
17/04/2023	v1.1	João Campos	Change the host designation to PNDC. Inclusion of a Line-Line fault plot in subsection 4.1.3. Change the column labels in tables 4 and 5.

Table of Contents

List of Figures

List of Tables

List of Abbreviations

DSO	Distribution System Operator
KPI	Key Performance Indicator
LG	Line-Ground
LL	Line-Line
LLG	Line-Line-Ground
LLL	Line-Line-Line
LLLG	Line-Line-Line-Ground
SRM	Simple Reactance Method
LV	Low Voltage
TDR	Time Domain Reflectometry
LA	Lab Access
UP	User Project

Executive Summary

There are currently several fault monitoring systems in the LV network. However, their cost is often high and their installation/operation is not always straightforward, making it difficult to obtain information in a short time span, impacting the decision time. Thus, to alleviate this issue, we developed a sensor that gathers the necessary data and sends it to a server so that our web application is able to calculate the impedance and distance to the fault.

The purpose of this work is to take advantage of the data given by the sensor to classify a fault into 5 categories: LG, LL, LLG, Line-Line-Line (LLL), Line-Line-Line-Ground (LLLG) and, with this information, obtain the impedance and distance to the fault, thus decreasing the time needed to pinpoint a fault and correct the issue. This is paramount to Distribution System Operator (DSO)'s as they may be penalized by the regulator if their Key Performance Indicator (KPI)'s deteriorate, being the time the service is down the most important one.

There are currently several methods to detect and locate faults. In the present work we focus on impedance based methods, which require the voltage and current phasors before and during the fault. These methods can be broadly divided in two groups: single-ended and double-ended methods. In the former, the currents and voltages are measured at one end of the cable and, in the latter, these variables are measured at both ends.

In order to assess our method's performance, we carried out experiments at the PNDC, in which controlled short-circuits were induced in PNDC's LV network. The experiments consisted in inducing LG, LL, LLG, LLL and LLLG faults in two different positions for 5 different resistances (0Ω, 0.75Ω, 5Ω, 10Ω, 20Ω) in a total of 50 experiments.

Impedance methods assume a clear distinction between the current before and after the fault. As the fault resistance increases, both become increasingly similar, which prevents any impedance based algorithm from giving an accurate distance estimation. Thus, a total of 20 experiments were considered: 10 corresponding to a fault resistance of 0Ω and 10 corresponding to a fault resistance of 0.75Ω. We used the relative error to assess the algorithm's performance.

We wanted to assess the following metrics:

- M1: Percentage of fault events detected;
- M2: Percentage of fuse blown events detected;
- M3: Percentage of faults correctly classified;
- M4: Impedance relative error;
- M5: Distance relative error.

Considering metrics M1 and M2, the algorithm was able to detect 100% of the fault events (M1) and 100% of the fuse blown events (M2). This includes all the fault resistances mentioned above, from 0Ω to 20Ω.

Concerning metrics M3-M5, these were only defined for fault resistances of 0Ω and 0.75Ω and do not apply to the 5Ω, 10Ω and 20Ω fault tests. This is due to the fact that the increase in the fault resistance leads to current values in the same order of magnitude before and during the fault, which is highly detrimental to the performance of impedance-based methods. However, these events were detected by the Eneida DTVI and the waveform data was gathered for future analysis, as we plan to cover these higher impedance faults with a different approach.

For the fault resistances considered (0Ω and 0.75Ω), the algorithm correctly classified 100% of the faults (M3).

Considering M4, we obtained 7/10 (70%) events with a relative error lower than the maximum admissible relative error defined (15%) for a fault resistance of 0Ω, the median relative error was 11.37% and the maximum relative error was 27.51%. For a fault resistance of 0.75Ω all the events were below the maximum admissible relative error defined (50%), the median of the relative error was 2.49% and the maximum relative error was 6.14%.

As for M5, we obtained 6/10 (60%) events with a relative error lower than the maximum admissible relative error defined (15%) for a fault resistance of 0Ω, the median relative error was 11.35% and the maximum relative error was 21.81%. For a fault resistance of 0.75Ω 9/10 (90%) events presented a relative error lower than the maximum admissible relative error defined (50%), the median relative error was 20.88%, and the maximum relative error was 53.62%.

It was also within the scope of this work to assess whether the defined acceptance criteria were appropriate to evaluate the performance. The results indicate that while metrics M1-M3 were well defined, metrics M4 and M5 were not adequate to obtain a clear understanding of the performance of the algorithms. The success criteria defined for distance (M5) were set as a relative error, this implies that the absolute error increases with the distance to the fault, which was not confirmed by the test results. For 0Ω faults, 9 out of 10 tests present an absolute error of less than 100m. For 0.75Ω faults, 8 out of 10 tests have an absolute error under 200m. In both cases, an outlier was registered for a distance of 897.5m to the fault. For these outliers, at 0Ω fault impedance, the absolute error was in the order of 200m, while for 0.75Ω it increased to around 300m.

1 Lab-Access User Project Information

1.1 Overview

User Project Title:	Fault TroubleShooter
User Project Acronym:	FaultTS
Host Infrastructure:	PNDC
Access Period:	7th February 2023 - 10th February 2023
User Group Members:	José Oliveira, Guilherme Freire, João Campos

1.2 Research Motivation, Objectives, and Scope

The motivation behind this research project is the fact that it is currently difficult for DSO's to pinpoint a fault as standard methods either imply the deployment of a field team to search for the fault's location, which is time consuming, or the use of methods that are usually costly.

The objective is to test a pipeline where the fault is detected, classified and located. The scope of the project is within protection systems in the LV network.

1.3 Structure of the Document

This document is organised as follows: Section 2 briefly outlines the state-of-the-art/state-of-technology that provides the basis of the realised Lab Access (LA) User Project (UP). Section 3 briefly outlines the performed experiments whereas Section 4 summarises the results and conclusions. Potential open issues and suggestions for improvements are discussed in Section 5.

2 State-of-the-Art/State-of-Technology

A fault on the LV network can severely disrupt the everyday life of people that rely on it. The longer the service remains down, the likelier it becomes that the DSO will receive complaints from customers and face consequences from the regulator. Thus, the location of a fault becomes a crucial problem that has been tackled in different ways.

Time Domain Reflectometry (TDR) [5], [6], the Murray Loop Bridge [3], gas detection [1] and impedance methods [2], [4], [7] are ordinary techniques used to pinpoint a fault. They differ in the underlying technology used, their price and accessibility.

TDR consists in injecting a pulse at the end of a cable and measuring the time until its reflection returns.

When using the Murray Loop Bridge technique, one end of the cable is shunted and two known resistances are connected at the other end. By calibrating the two resistances until they are subject to the same voltage difference, it is possible to obtain the distance to the fault.

When a fault occurs, the cable's insulator is damaged and liberates gases. By drilling small holes on the ground and using a cable sniffer, it is possible to detect the increased gas concentration as the fault location is nearer.

There are several impedance-based methods available [2]. They rely on being able to calculate the current and voltage phasors before and during the fault. They are usually divided in two groups: single-ended, when the voltage and current are measured at only one end of the cable, and double-ended, when measurements are performed at both ends.

Double-ended methods typically yield better results. However, they require more measuring devices, which can be costly, and increase the number of potential failure points. The solution we aimed to test within the scope of this project is based on single-ended methods.

The main single-ended impedance methods are the Simple Reactance Method (SRM), the Takagi method and its variations [2], [7]. They rely on similar assumptions but vary in the way they handle the fault resistance, whether they take the load into consideration by taking into account the pre-fault current and how they address the lack of system homogeneity [4], [2].

SRM assumes a purely resistive fault resistance it provides an estimate to the fault's distance using the imaginary part of the fault impedance seen from the fault and the cable's impedance. The Takagi method compensates the load current by subtracting the pre-fault current phasor to the fault current phasors.

3 Executed Tests and Experiments

3.1 Test Plan, Standards, Procedures, and Methodology

The test plan aims to induce short-circuits in positions D2 and A1 of the setup. The short-circuits induced will be of different 5 fault types: LG, LL, LLG, LLL, LLLG, with 5 different resistances 0Ω, 0.75Ω, 5Ω, 10Ω, 20Ω.

The current and voltage were measured during the faults in positions F2 using our device (DTVI) and a Fluke. The voltages and currents were also measured in position A1 using a Fluke. Both Fluke devices were supplied by PNDC. While the fluke measures were useful to compare with the signals obtained by the DTVI, only the signals obtained by our device were used to obtain the results.

The sampling rate of the DTVI was set to 4kHz.

3.2 Test Set-up(s)

The following test setup was used to carry out different experiments:

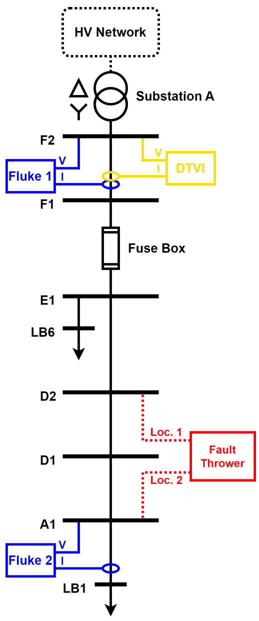

Figure 1: Setup used for the experiments.

3.3 Data Management and Processing

The DTVI device sent the data to Eneida Deepgrid® - Eneida's web platform - where the waveform data was stored in a database for later analysis. The Fluke devices recorded their data in csv files and were stored to confirm the wave forms sent by the DTVI.

4 Results and Conclusions

The following metrics were considered for the tests results:

- M1: Percentage of fault events detected;
- M2: Percentage of fuse blown events detected;
- M3: Percentage of faults correctly classified;
- M4: Impedance relative error;
- M5: Distance relative error.

For metrics M3-M5, we considered the following fault resistances: 0Ω and 0.75Ω as for resistances above these, impedance based methods would not yield sound results.

4.1 Discussion of Results

4.1.1 Percentage of fault events detected

During the tests, all the faut events caused on the network were correctly detected by the Eneida DTVI and shown in Eneida DeepGrid®. Thus, the value obtained for metric M1 is 100%. It should be noted that one of the main goal of this project was to test whether the solution was capable of consistently detecting short-circuit events. However, it was not within the scope of this project to test events that could potentially generate false positives in the fault detection method. Thus, this accuracy of 100% should be interpreted strictly within the proposed set of short-circuit tests. Therefore, metric M1 indicates that no false positives were detected, but is not adequate to give an indication regarding false positives.

The figure below is an example of the waveform data gathered for one of the fault events (0Ω fault between L1 and Ground, on position D2).

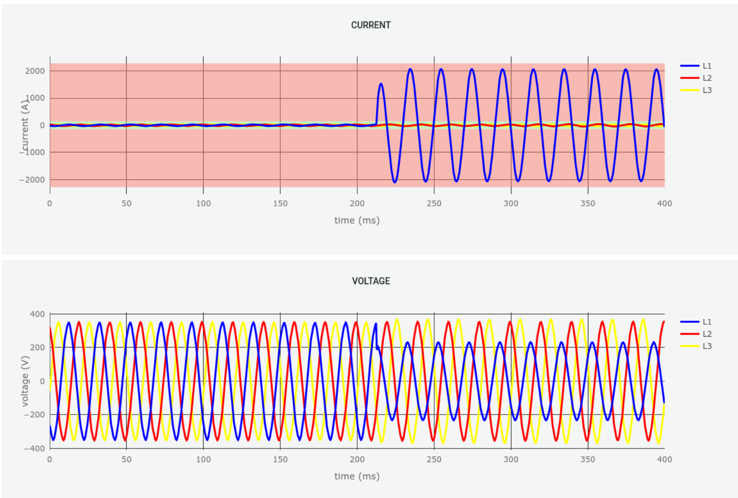

Figure 2: Fault event for a fault LG on position D2 (0Ω).

4.1.2 Percentage of fuse blown events detected

Similarly to what was observed for the fault events, all the fuse blown events that cleared the faults were also captured. Therefore, the value obtained for metric M2 is also 100%. Similarly to metric M1, this 100% accuracy refers strictly to the proposed set of short-circuit tests, since it was not within the scope of this project to test events that could generate false positive in the fuse blown detection method.

The figure below is an example of the waveform data gathered for one of the detected fuse blown events (fuse blown event on L1 corresponding to the fault event shown on the previous section).

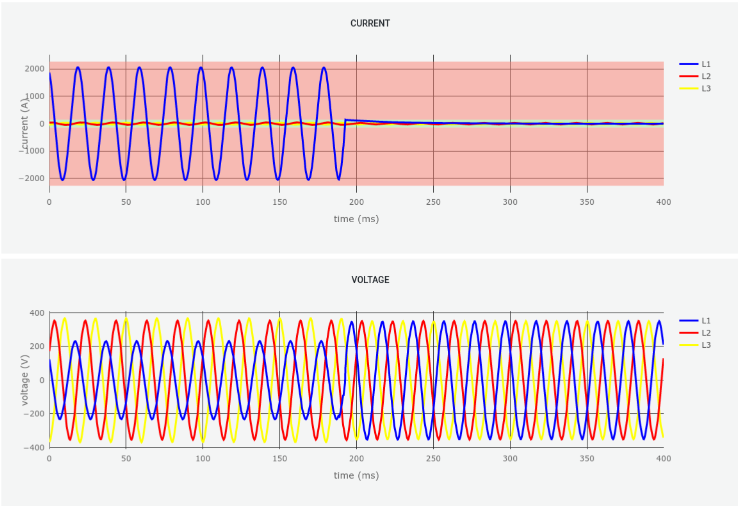

Figure 3: Fuse blown event corresponding to the fault event shown in fig. 2.

4.1.3 Percentage of faults correctly classified

In the following section we compare the real phases with the classification obtained by the algorithm (tables 1 and 2). The labels are as follows:

- L1: Phase 1,
- L2: Phase 2,
- L3: Phase 3,
- G: Ground.

When two faults are connected to a single point, the currents are reconfigured to make the current null in the connection point. Therefore, in LL faults, the currents of the fault events will present a phase difference of 180º, making the distinction between LL and LLG faults relevant (figures 4 and 5). This phenomenon will not be observed when comparing LLL/LLLG faults.

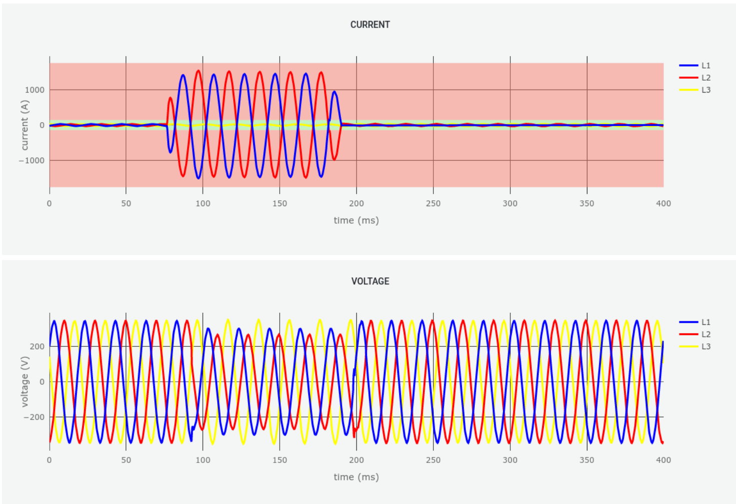

Figure 4: Currents and voltages for a LL fault between phases L1 and L2 (fault impedance: 0Ω) in position A1.

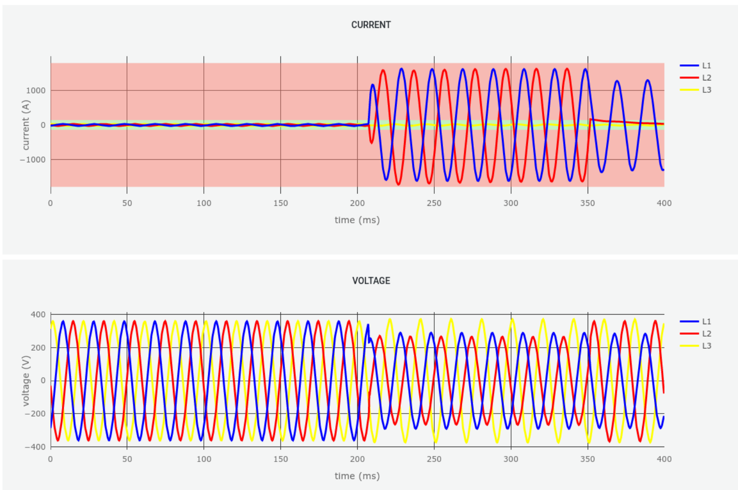

Figure 5: Currents and voltages for a LLG fault between phases L1 and L2 and ground (fault impedance: 0Ω) in position A1.

Table 1: Fault Classification (0Ω).

Fault Type	Phases	Network Point	Distance (m)	Classification
LG	[L1,G]	D2	377.5	[L1,G]
LL	[L2,L3]	D2	377.5	[L2,L3]
LLG	[L2,L3,G]	D2	377.5	[L2,L3,G]
LLL	[L1,L2,L3]	D2	377.5	[L1,L2,L3]
LLLG	[L1,L2,L3,G]	D2	377.5	[L1,L2,L3]
LG	[L1,G]	A1	897.5	[L1,G]
LL	[L1,L2]	A1	897.5	[L1,L2]
LLG	[L1,L2,G]	A1	897.5	[L1,L2,G]
LLL	[L1,L2,L3]	A1	897.5	[L1,L2,L3]
LLLG	[L1,L2,L3,G]	A1	897.5	[L1,L2,L3]

Table 2: Fault Classification (0.75Ω).

Fault Type	Phases	Network Point	Distance (m)	Classification
LG	[L1,G]	D2	377.5	[L1,G]
LL	[L1,P2]	D2	377.5	[L1,L2]
LLG	[L2,L3,G]	D2	377.5	[L2,L3,G]
LLL	[L1,L2,L3]	D2	377.5	[L1,L2,L3]
LLLG	[L1,L2,L3,G]	D2	377.5	[L1,L2,L3]
LG	[L1,G]	A1	897.5	[L1,G]
LL	[L1,L2]	A1	897.5	[L1,L2]
LLG	[L1,L2,G]	A1	897.5	[L1,L2,G]
LLL	[L1,L2,L3]	A1	897.5	[L1,L2,L3]
LLLG	[L1,L2,L3,G]	A1	897.5	[L1,L2,L3]

Table 3: Classification Accuracy.

Fault Resistance (Ω)	Acceptance Criterion	Number of Total Events	Number of Events Correctly Classified	Accuracy (%)
0	$\leq$ 90% PASS $>$ 90% FAIL	10	10	100
0.75	$\leq$ 90% PASS $>$ 90% FAIL	10	10	100

4.1.4 Impedances

Tables 4 and 5 present the impedances to fault obtained by our algorithm and their relative error. We then present the success criteria for the fault impedances (table 6) and the final results concerning the impedances to fault (tables 7 and 8).

Table 4: Impedances to fault for a fault impedance of 0Ω.

Fault Type	Network Point	Impedance to Fault (Ω)	Estimated Impedance to Fault (Ω)	Relative Error(%)
LG	D2	0.0874	0.1115	27.51
LL	D2	0.0874	0.0787	-9.99
LLG	D2	0.0874	0.0801	-8.42
LLL	D2	0.0874	0.0763	-12.73
LLLG	D2	0.0874	0.0849	-2.87
LG	A1	0.1801	0.2224	23.44
LL	A1	0.1801	0.1546	-14.17
LLG	A1	0.1801	0.1517	-15.79
LLL	A1	0.1801	0.1665	-7.56
LLLG	A1	0.1801	0.1621	-10.02

Table 5: Impedances to fault for a fault impedance of 0.75Ω.

Fault Type	Network Point	Impedance to Fault (Ω)	Estimated Impedance to Fault (Ω)	Relative Error(%)
LG	D2	0.8330	0.8841	6.14
LL	D2	0.8330	0.8576	2.96
LLG	D2	0.8330	0.8544	2.56
LLL	D2	0.8330	0.8778	5.38
LLL	D2	0.8330	0.8531	2.41
LG	A1	0.9196	0.9711	5.60
LL	A1	0.9196	0.9294	1.06
LLG	A1	0.9196	0.9280	0.92
LLL	A1	0.9196	0.9354	1.72
LLL	A1	0.9196	0.9401	2.23

Table 6: Success Criteria for Impedance to Fault.

Fault Impedance (Ω)	Success Criterion
0	$\leq$ 15% PASS $>$ 15% FAIL
0.75	$\leq$ 50% PASS $>$ 50% FAIL

Table 7: Event Classification (Impedance to Fault).

Fault Impedance (Ω)	Acceptance Criterion	Number of Total Events	Number of Successful Events
0	$\leq$ 15% PASS	10	7
0.75	$\leq$ 50% PASS	10	10

Table 8: Error Comparison (Impedance to Fault)

Fault Impedance(Ω)	Min. Rel. Error (%)	Median Rel. Error (%)	Max. Rel. Error (%)
0	2.87	11.37	27.51
0.75	0.92	2.49	6.14

4.1.5 Distances

Tables 9 and 10 present the distances obtained by our algorithm, their relative error and the difference to the actual distance. We then present the success criteria for the distances (table 11) and the final results concerning the distance (tables 12 and 13).

Table 9: Fault Distances (0Ω).

Fault Type	Network Point	Distance (m)	Estimated Distance (m)	Relative Error(%)	Distance Difference (m)
LG	D2	377.5	389.6	3.21	12.1
LL	D2	377.5	450.3	19.29	72.8
LLG	D2	377.5	454.2	20.32	76.7
LLL	D2	377.5	438.6	16.19	61.1
LLLG	D2	377.5	422.1	11.82	44.6
LG	A1	897.5	701.7	-21.81	-195.8
LL	A1	897.5	849.1	-5.39	-48.4
LLG	A1	897.5	822.2	-8.39	-75.3
LLL	A1	897.5	799.8	-10.89	-97.7
LLLG	A1	897.5	827.4	-7.81	-70.1

Table 10: Fault Distances (0.75Ω).

Fault Type	Network Point	Distance (m)	Estimated Distance (m)	Relative Error(%)	Distance Difference (m)
LG	D2	377.5	579.9	53.62	202.4
LL	D2	377.5	564.7	49.59	187.2
LLG	D2	377.5	504.2	33.57	126.7
LLL	D2	377.5	419.6	11.16	42.1
LLLG	D2	377.5	433.7	14.87	56.2
LG	A1	897.5	711.6	-20.72	-185.9
LL	A1	897.5	809.9	-9.76	-87.6
LLG	A1	897.5	1086.4	21.04	188.9
LLL	A1	897.5	610.4	-31.99	-287.1
LLLG	A1	897.5	944.4	5.22	46.9

Table 11: Success Criteria for Distance.

Impedance to Fault (Ω)	Success Criterion
0	$\leq$ 15% PASS $>$ 15% FAIL
0.75	$\leq$ 50% PASS $>$ 50% FAIL

Table 12: Event Classification (Distances)

Fault Impedance (Ω)	Acceptance Criterion	Number of Total Events	Number of Successful Events
0	$\leq$ 15% PASS	10	6
0.75	$\leq$ 50% PASS	10	9

Table 13: Error Comparison (Distances)

Fault Impedance (Ω)	Min. Rel. Error (%)	Median Rel. Error (%)	Max. Rel. Error (%)
0	3.21	11.35	21.81
0.75	5.22	20.88	53.62

4.2 Conclusions

The ERIGrid 2.0 Lab Access programme was paramount to provide access to data from a more complex LV network. Regarding the performance of the impedance and distance to fault methods, for low fault resistances, while the 0.75Ω tests generally meet the defined acceptance criteria, a significant amount of the 0Ω tests falls outside these criteria. Three main reasons were identified:

- The lengths of the cables and the impedance per unit length used in the calculations are approximate values (the best estimate possible), and can, to some extent, introduce a small error in the results, which will be more evident in the 0Ω tests since the absolute values of the impedance are very low.
- The defined acceptance threshold of 15% relative error for 0Ω was too optimistic. As mentioned in the Executive Summary, it was also within the scope of this work to assess whether the success criteria were appropriate. These results reveal that metrics M4 and M5 were not adequate to obtain a clear understanding of the performance of the algorithms.
- The analysis of the results revealed that the relative error may not be the best metric to assess the performance of the methods under test. Thus, the absolute error would be more indicated. The acceptance criteria could have been defined as an absolute error lower than 100m for 0Ω tests and lower than 200m for 0.75Ω tests, with only 1 and 2 tests falling outside the acceptance criterion for 0Ω and 0.75Ω respectively. These are admissible thresholds even if, in some cases, they correspond to relative errors higher than the actual defined acceptance criterion of 15%.

The method will allow for much faster decision and narrow substantially the potential fault location without sending a team to pinpoint the fault at a lower cost than methods that use other techniques.

5 Open Issues and Suggestions for Improvements

One issue that remains open relates to the handling of fault location for relatively high fault impedances ($\geq 5\Omega$), where the fault current is only slightly higher than the load current. While for lower impedances the method shows a solid performance, in these cases, since the impedance of the network between the measurement point and the fault is residual when compared to the fault resistance, impedance based methods will typically yield inaccurate results. This is a limitation of this type of low-cost method which needs to be studied and, if possible, mitigated by complementary methods.

Although the current methods are considered to be a very solid basis, there is room for improvement. We believe that an active learning approach should be explored. Furthermore, the implementation of feedback loops is essential, since this will allow the methods to improve based on past performance and direct feedback from DSO's.

References

[1] Khalif H. Ali, Stephen Bradley, Ahmed A. Aboushady, Salah A. Abdel Maksoud, and Mohamed E. Farrag. Developing a framework for underground cable fault- finding in low voltage distribution networks. In *2020 9th International Conference on Renewable Energy Research and Application (ICRERA)*, pages 477–482, 2020.

[2] Swagata Das, Surya Santoso, Anish Gaikwad, and Mahendra Patel. Impedance-based fault location in transmission networks: theory and application. *IEEE Access*, 2:537–557, 2014.

[3] M. R. Hans, Snehal C. Kor, and A. S. Patil. Identification of underground cable fault location and development. In *2017 International Conference on Data Management, Analytics and Innovation (ICDMAI)*, pages 5–8, 2017.

[4] Felipe V. Lopes, Eduardo Jorge S. Leite Jr, João Paulo G. Ribeiro, Artur B. Piardi, Allan V. Scheid, Guilherme Zat, and Renzo G.F. Espinoza. Single-ended multi-method phasor-based approach for optimized fault location on transmission lines. *Electric Power Systems Research*, 212:108361, 2022.

[5] S. Navaneethan, J.J. Soraghan, W.H. Siew, F. McPherson, and P.F. Gale. Automatic fault location for underground low voltage distribution networks. *IEEE Transactions on Power Delivery*, 16(2):346–351, 2001.

[6] Marco Scarpetta, Maurizio Spadavecchia, Francesco Adamo, Mattia Alessandro Ragolia, and Nicola Giaquinto. Detection and characterization of multiple discontinuities in cables with time-domain reflectometry and convolutional neural networks. *Sensors*, 21(23), 2021.

[7] T. Takagi, Y . Yamakoshi, M. Yamaura, R. Kondow, and T. Matsushima. Development of a new type fault locator using the one-terminal voltage and current data. *IEEE Transactions on Power Apparatus and Systems*, PAS-101(8):2892–2898, 1982.

Disclaimer

This document contains material, which is copyrighted by the authors and may not be reproduced or copied without permission.

The commercial use of any information in this document may require a licence from the proprietor of that information.

Neither the Lab Access User Group as a whole, nor any single person warrant that the information contained in this document is capable of use, nor that the use of such information is free from risk. Neither the Lab Access User Group as a whole, nor any single person accepts any liability for loss or damage suffered by any person using the information.

This document does not represent the opinion of the European Community, and the European Community is not responsible for any use that might be made of its content.

Copyright Notice

This project has received funding from the European Union's Horizon 2020 research and innovation programme under Grant Agreement No. 870620.